Cervical Cord FMRI Abnormalities Differ Between the Progressive Forms of Multiple Sclerosis

Paola Valsasina,[1] Maria A. Rocca,[1,2] Martina Absinta,[1,2] Federica Agosta,[1,2] Domenico Caputo,[3] Giancarlo Comi,[2] and Massimo Filippi[1,2]*

[1]*Neuroimaging Research Unit, Institute of Experimental Neurology, Division of Neuroscience, Milan, Italy*
[2]*Department of Neurology, Scientific Institute and University Hospital San Raffaele, Milan, Italy*
[3]*Department of Neurology, Scientific Institute Fondazione Don Gnocchi, Milan, Italy*

Abstract: *Objective:* Aim of this study was to compare tactile-associated cervical cord fMRI activity between primary progressive (PP) and secondary progressive (SP) MS patients and to investigate whether cord recruitment was associated with structural brain and cord damage. *Experimental Design:* Cervical cord fMRI during a tactile stimulation of the right hand was acquired from 17 healthy controls, 18 SPMS patients, and 16 PPMS patients. Average fMRI activity and its topographical distribution in cord sectors (left vs. right, posterior vs. anterior) were assessed. Correlations between cord recruitment and structural cord and brain MRI were estimated. *Principal Observations:* Progressive MS patients showed an increased cord recruitment compared with controls ($P = 0.003$). Despite a similar structural cord damage, cord activity was increased in SPMS compared to PPMS patients ($P = 0.05$). Regional analysis showed a non-lateralized pattern of cord recruitment in MS patients. Compared to PPMS, SPMS patients had grey matter (GM) atrophy in several cortical and subcortical regions. In SPMS patients, atrophy of the left postcentral gyrus was correlated with cord activity ($r = -0.48$, $P = 0.04$). *Conclusions:* Patients with progressive MS had an over-recruitment of the cervical cord, which was more pronounced in SPMS than PPMS, despite similar cord structural damage. The alteration of the complex modulation of spinal cord interneurons possibly due to a loss of supratentorial inhibition secondary to brain injury might contribute to explain the observed functional cord abnormalities. *Hum Brain Mapp 33:2072–2080, 2012.*

Key words: primary progressive multiple sclerosis; secondary progressive multiple sclerosis; cervical cord; functional magnetic resonance imaging

INTRODUCTION

Chronic progressive multiple sclerosis (MS) may result from a steady deterioration from onset of the clinical symptoms (and such a condition is termed primary progressive [PP] MS) [Montalban et al., 2009] or it may follow an initial phase of relapses and remissions (secondary progressive [SP] MS) [Lublin and Reingold, 1996]. Because of the high sensitivity and specificity to the heterogeneous pathological substrates of MS, several advanced magnetic resonance imaging (MRI) techniques have been applied during the past few years in an attempt to characterize the different forms of progressive MS and, ultimately, to

*Correspondence to: Prof. Massimo Filippi, Neuroimaging Research Unit, Institute of Experimental Neurology (INSPE), Division of Neuroscience, Scientific Institute and University Hospital San Raffaele, via Olgettina 60, 20132 Milan, Italy.
E-mail: massimo.filippi@hsr.it

Received for publication 24 February 2011; Revised 24 March 2011; Accepted 11 April 2011

DOI: 10.1002/hbm.21346

Published online 25 August 2011 in Wiley Online Library (wileyonlinelibrary.com).

improve our understanding of the mechanisms related to the development of irreversible deficits in this condition. Seminal MRI studies of the brain have shown that the extent of T2-visible lesions is higher in SPMS than PPMS [Nijeholt et al., 1998; Thompson et al., 1991]; more recently, it has also been shown that the "diffuse" damage to the normal appearing (NA) white matter (WM) and grey matter (GM) is more severe in SPMS vs. PPMS [Rovaris et al., 2002; Vrenken et al., 2010]. On the contrary, imaging studies of the spinal cord demonstrated a similar involvement of this structure in the two progressive forms of the disease, in terms of focal lesions [Nijeholt et al., 1998], damage to normally appearing tissue [Agosta et al., 2007a; Rovaris et al., 2001], and atrophy [Agosta et al., 2007a; Losseff et al., 1996; Rovaris et al., 2001]. Although an extensive comparison of brain functional MRI (fMRI) activity between PPMS and SPMS during active tasks is still missing, there is some evidence that resting state brain activity is altered in both progressive MS phenotypes, and that the entity of such change is greater in SPMS than in PPMS [Rocca et al., 2010]. This might be coherent with the more severe brain damage in SPMS patients.

Despite being technically challenging, fMRI has been reliably applied to explore spinal cord function in healthy subjects [Agosta et al., 2009b; Maieron et al., 2007; Stroman, 2008] and MS patients during tactile and proprioceptive tasks [Agosta et al., 2008, 2009a; Valsasina et al., 2010]. In line with brain fMRI findings, we postulated that increased fMRI cord recruitment in SPMS vs. PPMS might also be detected in the cervical cord. However, given the similarity of these two disease phenotypes with respect to cord structural damage, we expected that such a difference might be related to the extent of brain rather than cervical cord structural damage. To test this hypothesis, we compared the extent and the topographical distribution of tactile-associated cervical cord fMRI activation in patients with PPMS and SPMS. To understand better the mechanisms responsible for abnormal cervical cord recruitment, we also assessed the correlation between the extent of fMRI activations and several MRI measures of brain and cord structural damage.

METHODS

Patients

We studied 34 right-handed [Oldfield, 1971] patients with definite and progressive MS. Eighteen patients had SPMS [Lublin and Reingold, 1996] and 16 had PPMS [Montalban et al., 2009]. The main demographic and clinical characteristics of these patients are shown in Table I. Two PPMS patients (6% of the study cohort) had a mild disability (expanded disability status scale [EDSS] score [Kurtzke, 1983] $\leq$3.5), whereas all remaining PPMS and SPMS patients (94%) had an EDSS score $\geq$4.0. To be included patients had to have: (1) no evidence of sensory impairment of the right, dominant upper limb; (2) no previous clinical episode attributable to the involvement of the cervical cord, such as acute myelitis, myelopathy, trauma, or other spinal diseases potentially affecting the cord; (3) no steroid therapy for at least six months prior to study entry; (4) no other major medical conditions; (5) no history of alcohol or drug abuse; and (6) no treatment with any psychoactive drug. Seventeen right-handed [Oldfield, 1971] healthy subjects (eight women and nine men; mean age = 49.6 years, SD = 9.3 years), with no previous history of neurological dysfunction and a normal neurological exam, served as controls.

TABLE I. Main demographic and clinical characteristics of the MS patients enrolled in this study

	All MS patients	SPMS patients	PPMS patients
Women/men	16/18	10/8	6/10
Mean age (SD) [years]	51.1 (9.4)	53.1 (8.5)	49.0 (10.1)
Median disease duration (range) [years]	16 (1–31)	20 (3–31)	8.5 (1–24)
Median EDSS (range) score	5.5 (3.0–6.5)	5.5 (4.0–6.5)	5.5 (3.0–6.5)

Abbreviations: MS = multiple sclerosis; SP = secondary progressive; PP = primary progressive; SD = standard deviation; EDSS = expanded disability status scale.

Standard Protocol Approvals and Patient Consents

Approval was received from local ethical standards committee on human experimentation and written informed consent was obtained from all patients participating into the study.

MRI Acquisition

MRI data were obtained using a 1.5 T Siemens scanner (Erlangen, Germany). Using a phased-array neck coil, cervical cord fMRI data were acquired with a multi-shot turbo spin-echo (TSE) sequence (TR/TE = 2850/11 ms; flip angle [FA] = 120°; field of view [FOV] = 100 × 100 mm^2; matrix = 256 × 244, in-plane resolution = 0.39 × 0.39 mm^2, turbo factor = 25). Nine contiguous axial slices (slice thickness = 7 mm), aligned with the vertebral body centers or with the intervertebral disks [Stroman et al., 2001], covering cord segments from C5 to T1, were acquired. Spatial saturation pulses anterior and posterior to the cord were used to avoid aliasing and to reduce motion artifacts from breathing and swallowing. Flow compensation in the slice direction was applied to reduce artifacts from cerebrospinal fluid (CSF) flow.

In the same scanning session, the following structural MRI scans were also obtained:

1. Cervical cord: (a) sagittal dual-echo TSE (TR/TE = 2,000/30–145 ms; FA = 150°; turbo factor = 23; FOV =

300 × 300 mm^2; matrix = 320 × 320; number of averages [NEX] = 1; seven slices with thickness = 4 mm); (b) sagittal T1-weighted 3D magnetization-prepared rapid acquisition gradient echo (MP-RAGE) (TR/TE = 1,160/4.2 ms; inversion time [TI] = 600 ms; FA = 15°; FOV = 300 × 300 mm^2; matrix = 230 × 230; NEX = 2; slab thickness = 80 mm); (c) modified sensitivity-encoded (mSENSE) diffusion-weighted single-shot SE echo planar imaging (EPI) (reduction factor = 2; TR/TE = 2,700/71 ms; FA = 90°; FOV = 240 × 180 mm^2; matrix = 192 × 144; pixel size = 1.25 × 1.25 mm^2; NEX = 4; five sagittal slices with thickness = 4 mm; 12 non-collinear diffusion directions; b-factor = 900 s mm^{-2}).

2. Brain: (a) dual-echo TSE (TR/TE = 3,460/27–109 ms; FA = 150°; turbo factor = 5; FOV = 250 × 250 mm^2; matrix = 256 × 256; 44 contiguous axial slices with thickness = 3 mm); (b) sagittal T1-weighted 3D MP-RAGE (TR/TE = 2,000/3.93 ms; TI = 900 ms; FA = 12°; FOV = 270 × 270 mm^2; matrix = 256 × 256; slab thickness = 187.2 mm); (c) mSENSE diffusion-weighted single-shot SE EPI (reduction factor = 2; TR/TE = 2,700/71 ms; FA = 90°; FOV = 240 × 240 mm^2; matrix size = 128 × 128; pixel size = 1.87 × 1.87 mm^2; NEX = 4; 18 axial slices with thickness = 4 mm; 12 non-collinear diffusion directions; b-factor = 900 s mm^{-2}).

fMRI Experimental Design

Using a block design (ABAB), where four periods of rest were alternated with four periods of activity (each period consisting of five scans), the subjects were scanned while administering a tactile stimulation of the palm of the right hand. During the stimulation periods, an observer inside the scanner room pushed and pulled a home-made device repeatedly tapping to the center of the palm of the subjects' right hand with the back side (∼ 1 × 1 cm^2) of a wooden spoon. The stimulus was paced by a metronome at 1 Hz frequency [Agosta et al., 2009b]. To prevent movements of the shoulder, arm, elbow, or forearm, subjects' arms were restrained with straps. The forearm was in a prone position with respect to the scanner table. Head motion was minimized using foam padding and ear blocks. Subjects were trained outside the scanner and were instructed to relax as much as possible and to keep their eyes closed during the entire duration of the experiment.

fMRI Analysis

All image post-processing was performed on an independent computer workstation (Sun Microsystem, Mountain View, CA) by an experienced observer blinded to subjects' identity. FMRI data were analyzed using a custom-made software written in MatLab (The MathWorks, Natick, MA). After extraction of cord tissue from the original images using the Jim software package (Version 5.0, Xinapse Systems, Northants, UK, http://www.xinapse.com), cord images were registered to the first scan by means of rigid-body translation and rotation, generating six motion parameters for each subject's scan. Maximum translation greater than 3.0 mm or maximum rotation greater than 0.04 radians in the x–y planes were considered as additional exclusion criteria (no patient was excluded for this reason). A band-pass filter was applied to the fMRI time-courses, to remove low-frequency drifts and high-frequency noise. No spatial smoothing was applied to the realigned scans to preserve the in-plane resolution and compensate for the small size of the cord. Transformed fMRI data were then analyzed using a General Linear Model (GLM) approach, consisting of a basis set composed of a box-car modeling the stimulus paradigm, a linear ramp to account for baseline trends, and a constant function to account for baseline intensity. Statistical t-maps were generated for all subjects ($P < 0.05$, uncorrected) and masked to retain only cord tissue. In each subject, the presence of fMRI activity at each cord level and quadrant was evaluated visually and each level/quadrant was defined as either "active" or "inactive." The mean signal intensity change induced by the task was also computed for all activated voxels within the cervical cord.

Cervical Cord Structural MRI Analysis

Cervical cord hyperintense lesions were identified on the sagittal DE scans. The diffusion tensor (DT) was calculated for each voxel of the cervical cord, and mean diffusivity (MD) and fractional anisotropy (FA) derived [Pierpaoli et al., 1996]. From MD and FA maps, the corresponding histograms were produced. Average cervical cord cross-sectional area (CSA) was assessed on MP-RAGE scans throughout the cord from C2 to C5 with a semi-automatic method based on an active surface model of the cord surface, as previously described [Horsfield et al., 2010]. CSA was normalized (CSAn) to the intra-cranial cross-sectional area, which was measured at the level of the inferior margins of the corpus callosum on an axial slice of the PD image, as described elsewhere [Horsfield et al., 2010], and the CSAn entered the statistical analysis.

Brain Structural MRI Analysis

Brain T2 lesion volumes (LV) were measured using the Jim software package. MD and FA maps were derived for each pixel. MD histograms of the NAWM and GM as well as FA histograms of the NAWM were produced, as previously described [Agosta et al., 2008]. On MP-RAGE images, intracranial volumes (ICV) were calculated using the structural imaging evaluation of normalized atrophy (SIENAx) software [Smith et al., 2002]. Voxel-based morphometry (VBM) was performed to define the regional distribution of atrophy in the GM, using statistical parametric

TABLE II. Cervical cord and brain structural MR quantities in control subjects and patients with primary progressive (PP) and secondary progressive (SP) multiple sclerosis (MS)

	Control subjects	PPMS patients	SPMS patients	*P*-values[a]
Normalized cord cross-sectional area (SD) [mm^2]	82.6 (4.6)	70.4 (7.7)	69.6 (0.5)	<0.001
Cord average MD (SD) [$\times 10^{-3}$ mm^2 s^{-1}]	0.84 (0.09)	0.98 (0.07)	0.97 (0.12)	<0.001
Cord average FA (SD)	0.57 (0.06)	0.44 (0.05)	0.46 (0.05)	<0.001
Brain T2 LV (SD) (ml)	—	8.8 (11.2)	28.1 (19.3)	0.001[b]
Brain GM average MD (SD) [$\times 10^{-3}$ mm^2 s^{-1}]	0.89 (0.04)	0.94 (0.05)	0.98 (0.04)	0.001
Brain NAWM average MD (SD) [$\times 10^{-3}$ mm^2 s^{-1}]	0.77 (0.02)	0.78 (0.02)	0.82 (0.03)	<0.001
Brain NAWM average FA (SD)	0.40 (0.02)	0.38 (0.02)	0.34 (0.03)	<0.001
Normalized brain volume (SD) [ml]	1567 (79)	1527 (64)	1430 (67)	<0.001
GM volume (SD) [ml]	828 (59)	808 (73)	691 (80)	<0.001
WM volume (SD) [ml]	739 (38)	718 (28)	729 (67)	0.38

Abbreviations: MS = multiple sclerosis; SP = secondary progressive; PP = primary progressive; MD = mean diffusivity; FA = fractional anisotropy; SD = standard deviation; GM = grey matter; WM = white matter; NAWM = normal-appearing white matter; LV = lesion volume.
[a]ANOVA model adjusted for age.
[b]Mann-Withney U test.

mapping (SPM8) (http://www.fil.ion.ucl.ac.uk/spm/software) and the Diffeomorphic Anatomical Registration using Exponentiated Lie algebra (DARTEL) registration method [Ashburner, 2007], as described in detail elsewhere [Riccitelli et al., 2011]. Briefly, after segmentation of MP-RAGE images into GM, WM, and CSF, GM maps were normalized to the GM population-specific template generated by DARTEL [Ashburner, 2007]. Normalized images were then modulated to ensure preservation of the overall amount of GM tissue and smoothed with an 8-mm full-width at half maximum kernel.

Statistical Analysis

Univariate analyses of variance (ANOVA) corrected for subject's age or the Mann-Withney U test for non-parametric data were used to compare functional and structural MRI quantities between controls and MS patients, as well as between patient groups.

Using random effect logistic regression models, with the frequency of fMRI activity as the dependent variable and the subject as the grouping factor, the within-group differences in the occurrence of fMRI activity were evaluated in: (a) right vs. left cord, (b) anterior vs. posterior cord, and (c) among different cord levels.

GM volume differences between patients and healthy controls, as well as between PPMS and SPMS patients, were assessed using SPM8 and a full factorial design, including age, gender and total ICV as confounding covariates. Results of between-group comparisons exceeding a threshold of $P < 0.001$ (uncorrected for multiple comparisons) and a cluster extent of $k = 10$ voxels underwent a small volume correction (SVC) for multiple comparisons ($P < 0.05$, 10-mm radius).

Regional GM volumes significantly different among groups were extracted from the original GM maps with the Marsbar toolbox [Brett, 2002] and used for correlation analysis. Univariate correlations between fMRI and structural cord and brain MRI quantities, as well as between fMRI measures and clinical variables were assessed using the Sperman rank correlation coefficient.

RESULTS

No cervical cord lesions were seen on the conventional MR images from healthy controls, 12 SPMS and 12 PPMS patients. Ten (30%) patients had T2-visible cord lesions: six patients had one lesion (two SPMS and four PPMS) and four SPMS patients had two lesions. Structural MRI results of cervical cord and brain from the three study groups are reported in Table II. All structural MRI-derived quantities were statistically different among the three groups ($P < 0.001$), with the exception of WM volume. At post-hoc comparisons, all previous structural MRI quantities were significantly different between SPMS and PPMS patients taken separately vs. healthy controls (P ranging from <0.001 to 0.05). Cord DT-MRI metrics and CSAn did not differ between PPMS and SPMS. Conversely, the majority of brain MRI quantities were significantly more altered in SPMS than in PPMS patients with reference to controls: T2 LV, GM, and NAWM average MD were significantly higher, whereas NAWM average FA, NBV, and GM volumes were significantly lower in SPMS vs. PPMS (P values ranging from 0.001 to 0.04).

The results of VBM analysis are summarized in Table III and shown in Figure 1. Compared to healthy controls, both PPMS and SPMS had significant GM atrophy of the left (L) thalamus and L insula, of the bilateral cerebellum, and several regions in the frontal lobes, including the precentral gyrus and the premotor cortex, bilaterally. SPMS patients had additional areas of GM loss in the right (R) cingulate cortex, L superior frontal gyrus (SFG),

TABLE III. Regions of grey matter atrophy in PPMS and SPMS patients vs. healthy controls, and between SPMS vs. PPMS patients (small-volume corrected *P*-values)

	PPMS vs. healthy controls			SPMS vs. healthy controls			SPMS vs. PPMS		
Anatomical region	MNI space coordinates	*t* value	*P* value	MNI space coordinates	*t* value	*P* value	MNI space coordinates	*t* value	*P* value
Thalamus									
L	−14, −16, 10	3.3	0.05	−14, −8, −8	7.1	<0.001	−10, −22, −2	6.5	<0.001
R	—	—	—	12, −10, −4	6.1	<0.001	12, −14, −4	5.9	<0.001
Pallidus									
L	20, −6, −6	3.8	0.01	—	—	—	–	—	—
R	—	—	—	—	—	—	–	—	—
Putamen									
L	—	—	—	−24, 6, −4	4.6	0.002	−22, 8, 10	4.1	0.006
R	—	—	—	24, 4, −4	4.8	0.001	28, 2, −2	3.9	0.01
Precentral gyrus (BA4)									
L	−24, −28, 64	3.6	0.02	—	—	—	—	—	—
R	—	—	—	46, −18, 48	4.1	0.007	—	—	—
Premotor cortex (BA6)									
L	—	—	—	−38, 0, 44	3.6	0.02	−42, −2, 62	3.5	0.02
							−8, −6, 72	4.2	0.01
R	8, −10, 58	3.8	0.01	38, 14, 50	4.8	0.001	—	—	—
Postcentral gyrus (BA3)									
L	—	—	—	−40, −24, 46	4.5	0.003	−40, −24, 56	3.9	0.01
							−38, −32, 50	3.3	0.03
R	—	—	—	50, −16, 54	3.9	0.01	—	—	—
Paracentral lobule (BA6)									
L	—	—	—	−2, −34, 56	4.4	0.003	−4, −34, 56	4.1	0.007
SFG (BA8)									
L	—	—	—	−22, 12, 52	5.0	0.001	−26, 20, 56	3.8	0.005
Insula									
L	−36, 30, 0	3.5	0.02	−34, 26, 6	3.5	0.03	—	—	—
Dorsal ACC (BA32)									
R	—	—	—	0, 14, 46	3.9	0.01	—	—	—
Dorsal PCC (BA31)									
R	—	—	—	14, −42, 34	3.8	0.01	—	—	—
Cerebellum (lobule VI)									
L	—	—	—	−22, −74, −18	4.2	0.005	—	—	—
R	26, −64, −28	3.3	0.04	28, −64, −26	3.3	0.04	—	—	—

Abbreviations: PPMS = primary progressive multiple sclerosis; SPMS = secondary progressive multiple sclerosis; L = left; R = right; BA = Brodmann area; SFG = superior frontal gyrus; ACC = anterior cingulate cortex; PCC = posterior cingulate cortex.

postcentral gyrus, and L paracentral lobule. Atrophy of the thalami and basal ganglia, bilaterally, L premotor cortex, L postcentral gyrus, L paracentral lobule, and L SFG was more pronounced in SPMS vs. PPMS patients.

Activity of the cervical cord from C5 to T1 was detected in all study subjects (Figs. 2 and 3). The mean signal intensity change of all activated voxels within the cervical cord was 2.65% (SD = 0.76%) in control subjects, 3.97% (SD = 1.26%) in SPMS patients, and 3.27% (SD = 0.56%) in PPMS patients (ANOVA, $P = 0.003$). Activation remained significantly different among groups also after correcting for CSAn ($P = 0.009$). Compared with controls, both SPMS ($P = 0.01$) and PPMS ($P = 0.02$) patients experienced a significantly increased cord fMRI recruitment. Cord activity was higher in SPMS than PPMS patients ($P = 0.05$). Mean cord signal intensity change did not differ between MS patients with and without T2 cord lesions ($P = 0.20$). In patients with MS, no correlation was found between mean cord signal intensity change and clinical measures (disease duration and EDSS), as well as with cervical cord and brain structural MRI quantities. In SPMS patients, fMRI cord activity was correlated only with atrophy of the L postcentral gyrus ($r = -0.48$, p = 0.04) (Fig. 4). In PPMS, cord fMRI activity did not correlate with brain regional GM atrophy.

In healthy subjects, the random effect logistic model showed a higher occurrence of fMRI activity in the

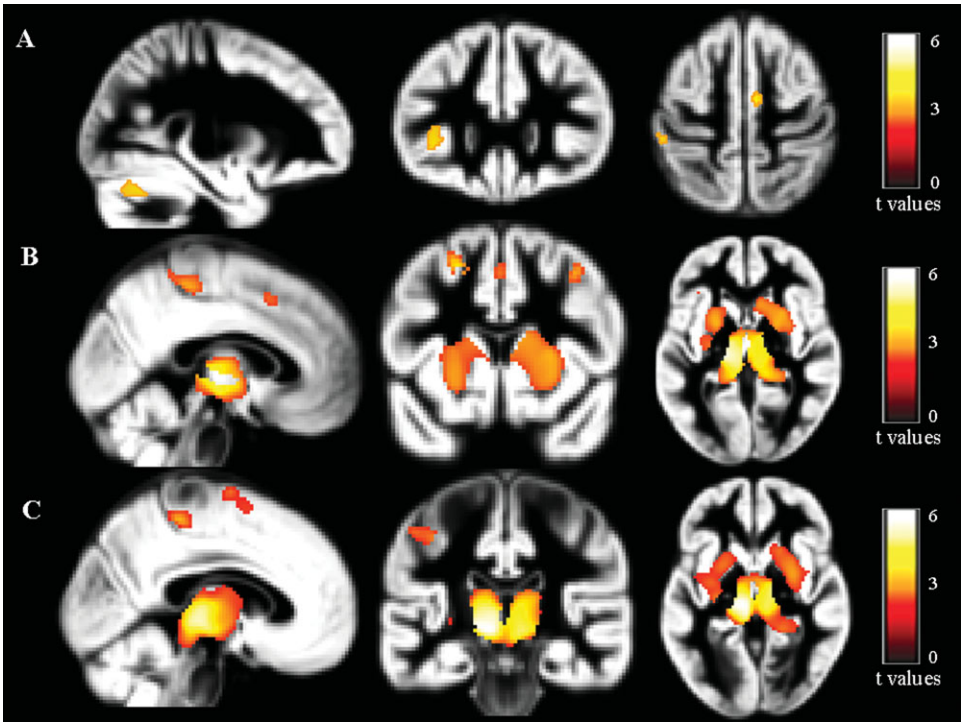

Figure 1.

Statistical parametric mapping (SPM) regions of gray matter (GM) loss superimposed on the customized GM template, contrasting primary progressive (PP) multiple sclerosis (MS) patients, secondary progressive (SP) MS patients, and healthy controls (HC) at a threshold of $P < 0.001$, uncorrected. A: PPMS patients *vs.* healthy controls; B: SPMS patients *vs.* healthy controls; and C: SPMS vs. PPMS patients. Images are in neurological convention.

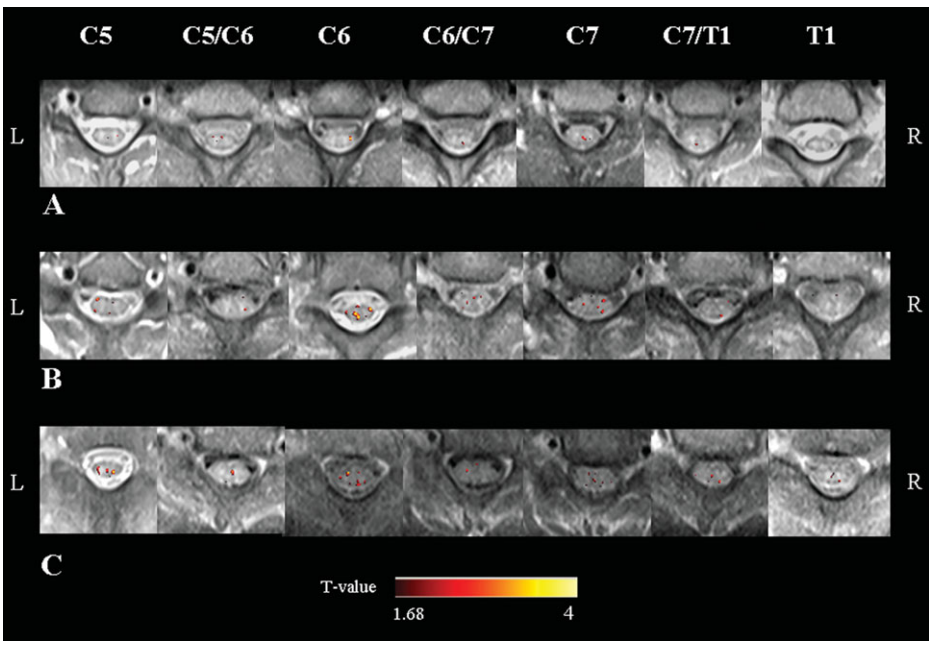

Figure 2.

Illustrative activation maps (color-coded for t values) of cervical cord on axial proton-density weighted spin-echo images from C5 to T1, from a healthy volunteer (A), a patient with primary progressive (PP) multiple sclerosis (MS) (B), and a patient with secondary progressive (SP) MS (C) during a tactile stimulation of the palm of the right hand. R: right, L: left.

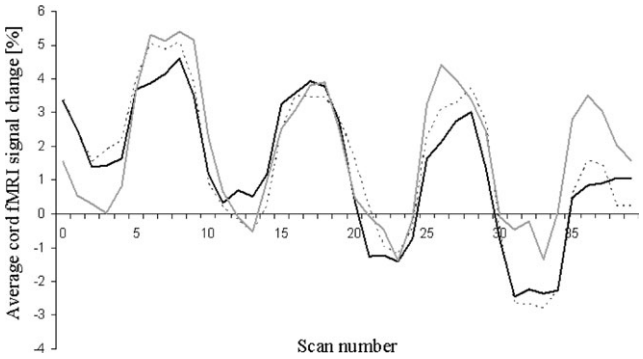

Figure 3.

Cervical cord average signal change during the tactile stimulation of the palm of the right hand in healthy controls (black line), patients with primary progressive multiple sclerosis (PPMS) (dotted grey line), and patients with secondary progressive multiple sclerosis (SPMS) (continuous grey line). See text for formal statistical analysis.

posterior *vs.* anterior (odds ratio [OR] = 0.43, 95% confidence intervals [CI] = 0.28–0.67, $P < 0.001$) and in the right vs. left (OR = 2.19, 95% CI = 1.41–3.39, $P < 0.001$) quadrants of the cord. Progressive MS patients (both considered as a whole group or separately) had no difference in the occurrence of posterior vs. anterior, or right vs. left activity. The within-group analysis showed that the occurrence of fMRI activity was significantly different among cord levels ($P < 0.001$), with a higher activity at C6 ($P < 0.001$) and C7 ($P < 0.001$), and lower activity at C7/T1 ($P = 0.001$). Such a distribution did not differ among the three groups ($P = 0.16$).

DISCUSSION

In this study, we assessed whether tactile-associated cervical cord fMRI activity differs between PPMS and SPMS patients and whether it is associated with cord and brain structural injury. Despite the technical challenges related to spinal cord fMRI, including the small size of the target structure and its proximity to bone, cartilage and CSF (with the potential bias introduced by partial volume effects), susceptibility artifacts and physiological noise [Stroman 2008], previous studies showed the ability of cord fMRI to detect abnormal patterns of recruitment in PPMS and SPMS patients considered separately, with respect to healthy controls [Agosta et al., 2009a; Valsasina et al., 2010]. To our knowledge, a direct comparison of cord fMRI recruitment between the two progressive forms of MS has not been performed yet. Such an investigation should result in a more complete picture of cord damage and function in MS patients with predominant locomotor deficits, which are likely linked to injury and dysfunction of this clinically eloquent structure.

The main result of this study is the demonstration that cord recruitment is increased in progressive MS patients vs. controls and, more importantly, in SPMS vs. PPMS patients, even if cord structural injury in these two patient cohorts was not different. The notion that the extent of structural cervical cord damage does not differ among the progressive phenotypes of MS is in agreement with the results of previous studies [Agosta et al., 2007a; Kidd et al., 1996; Nijeholt et al., 1998], but not with those of others [Losseff et al., 1996; Rovaris et al., 2001], which found a more severe cervical cord atrophy in SPMS than PPMS patients. Nonetheless, the rate of cord atrophy development was shown to be similar between the two progressive disease courses [Agosta et al., 2007a]. Quantitative MRI studies confirmed only a limited difference in cord injury between the two progressive MS phenotypes; one cross-sectional study showed a lower cord magnetization transfer ratio (MTR) in SPMS than PPMS [Rovaris et al., 2001], but a longitudinal study demonstrated a higher rate of FA decrease in PPMS than in SPMS patients over a follow-up of 2.5 years [Agosta et al., 2007a].

The similarity of structural cord abnormalities found in our patient groups, combined with the lack of a difference in the extent of cord fMRI recruitment between patients with and without cord T2 lesions, supports the notion that the increased cord activity observed in SPMS compared with PPMS is likely not to be the mere consequence of an overall greater focal cord damage. As a consequence, it is tempting to speculate that SPMS cord over-recruitment, which is likely secondary to an alteration of the complex excitatory and inhibitory modulation of spinal cord interneurons [Brodal, 1981; Kandel, 1991], might be due an altered supraspinal modulation. To investigate this hypothesis, we assessed the correlation between cord fMRI activity and structural brain damage in our patients. The

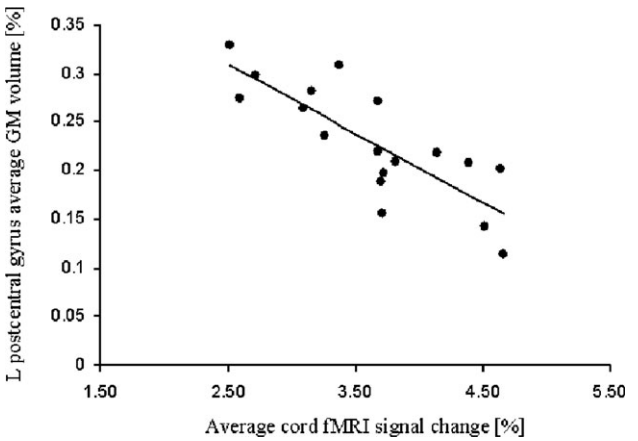

Figure 4.

Scatter plot of the correlation between cord fMRI average signal change and brain grey matter (GM) volume in the left (L) postcetral gyrus in secondary progressive multiple sclerosis (SPMS) patients.

quantification of structural brain injury showed that the extent of focal and diffuse damage was more severe in patients with SPMS in comparison with those with PPMS. Again, these findings are in line with those from previous studies, which showed that, when contrasted to PPMS, SPMS patients have a higher brain T2 lesion burden [Nijeholt et al., 1998], more severe microstructural brain injury [Rovaris et al., 2002; Vrenken et al., 2010], and more extensive GM loss [Ceccarelli et al., 2008], which involves regions with a critical role for sensorimotor integration, such as the thalami, basal ganglia, and several cortical regions in the frontal and parietal lobes. Remarkably, in our SPMS cohort, cord fMRI abnormalities were correlated significantly with brain GM tissue loss in the left postcentral gyrus, a key region for sensory stimuli processing, whereas regions of GM atrophy in PPMS did not correlate with fMRI cord activity. This finding suggests that the cord functional over-recruitment observed in SPMS with respect to PPMS might be explained, at least partially, by a loss of supratentorial inhibition following brain injury. Clearly, an additional and not mutually exclusive explanation of the observed fMRI abnormalities might be also due to damage to cord GM, which has been shown by pathologic [Gilmore et al., 2009], MR spectroscopy [Kendi et al., 2004] and MT MRI [Agosta et al., 2007b; Zackowski et al. 2009] studies. Unfortunately, to limit the amount of time that these disabled patients had to spend inside the scanner, we did not investigate this aspect and, as a consequence, we can not prove or disprove this hypothesis.

To characterize better spinal cord functional abnormalities, we also assessed the topographical distribution of cervical cord activity in the three study groups. Consistent with the expected regions of neuronal involvement for a tactile stimulation of the palm of right hand, healthy controls had a functional lateralization of cord activity, which was predominant in the cord side ipsilateral to the side where stimulus was delivered and in the posterior quadrants. Conversely, both PPMS and SPMS patients had a widespread pattern of recruitment, with loss of the physiologic asymmetries of activations observed in healthy individuals. This "diffuse" cord recruitment in MS patients is also in keeping with an altered function of cord interneurons [Brodal, 1981; Kandel, 1991]. Remarkably, such a diffuse and bilateral cord recruitment in progressive MS patients mirrors the results of previous fMRI studies of the brain, which showed that during the performance of a simple motor task these patients have a more extensive and bilateral pattern of cortical activation when compared to controls [Rocca et al., 2003] or to relapsing-remitting MS patients [Rocca et al., 2005].

In the entire group of MS patients, no correlation was found between cord fMRI findings and clinical disability. This was not unexpected considering the narrow range of disabilities of our patients. Indeed, two previous studies in relapse-onset [Valsasina et al., 2010] and progressive-onset [Agosta et al., 2009a] MS, described an increased cord recruitment in patients with severe clinical disability (EDSS $\geq$4.0) vs. patients with mild (EDSS $\leq$3.5) disability and vs. healthy controls.

REFERENCES

Agosta F, Absinta M, Sormani MP, Ghezzi A, Bertolotto A, Montanari E, Comi G, Filippi M (2007a): In vivo assessment of cervical cord damage in MS patients: A longitudinal diffusion tensor MRI study. Brain 130 (Part 8):2211–2219.

Agosta F, Pagani E, Caputo D, Filippi M (2007b): Associations between cervical cord gray matter damage and disability in patients with multiple sclerosis. Arch Neurol 64:1302–1305.

Agosta F, Valsasina P, Rocca MA, Caputo D, Sala S, Judica E, Stroman PW, Filippi M (2008): Evidence for enhanced functional activity of cervical cord in relapsing multiple sclerosis. Magn Reson Med 59:1035–1042.

Agosta F, Valsasina P, Absinta M, Sala S, Caputo D, Filippi M (2009a): Primary progressive multiple sclerosis: Tactile-associated functional MR activity in the cervical spinal cord. Radiology 253:209–215.

Agosta F, Valsasina P, Caputo D, Rocca MA, Filippi M (2009b): Tactile-associated fMRI recruitment of the cervical cord in healthy subjects. Hum Brain Mapp 30:340–345.

Ashburner J (2007): A fast diffeomorphic image registration algorithm. Neuroimage 38:95–113.

Brett M, Anton JL, Valabregue R, Poline JB (2002): Region of interest analysis using an SPM toolbox. 8th International Conference of Functional Mapping of the Human Brain, Sendai, Japan, Vol. 16. pp 2.

Brodal A (1981): Neurological Anatomy in Relation to Clinical Medicine. New York: Oxford University Press.

Ceccarelli A, Rocca MA, Pagani E, Colombo B, Martinelli V, Comi G, Filippi M (2008): A voxel-based morphometry study of grey matter loss in MS patients with different clinical phenotypes. Neuroimage 42:315–322.

Gilmore CP, DeLuca GC, Bo L, Owens T, Lowe J, Esiri MM, Evangelou N (2009): Spinal cord neuronal pathology in multiple sclerosis. Brain Pathol 19:642–649.

Horsfield MA, Sala S, Neema M, Absinta M, Bakshi A, Sormani MP, Rocca MA, Bakshi R, Filippi M (2010): Rapid semi-automatic segmentation of the spinal cord from magnetic resonance images: Application in multiple sclerosis. Neuroimage 50:446–455.

Kandel E, Schwartz J, Jessell TM (1991): Principles of Neural Science. Appleton & Lange. Norwalk, CT.

Kendi AT, Tan FU, Kendi M, Yilmaz S, Huvaj S, Tellioglu S (2004): MR spectroscopy of cervical spinal cord in patients with multiple sclerosis. Neuroradiology 46:764–769.

Kidd D, Thorpe JW, Kendall BE, Barker GJ, Miller DH, McDonald WI, Thompson AJ (1996): MRI dynamics of brain and spinal cord in progressive multiple sclerosis. J Neurol Neurosurg Psychiatry 60:15–19.

Kurtzke JF (1983): Rating neurologic impairment in multiple sclerosis: An expanded disability status scale (EDSS). Neurology 33:1444–1452.

Losseff NA, Webb SL, O'Riordan JI, Page R, Wang L, Barker GJ, Tofts PS, McDonald WI, Miller DH, Thompson AJ (1996): Spinal cord atrophy and disability in multiple sclerosis. A new reproducible and sensitive MRI method with potential to monitor disease progression. Brain 119 (Part 3):701–708.

Lublin FD, Reingold SC (1996): Defining the clinical course of multiple sclerosis: Results of an international survey. National multiple sclerosis society (USA) advisory committee on clinical trials of new agents in multiple sclerosis. Neurology 46:907–911.

Maieron M, Iannetti GD, Bodurka J, Tracey I, Bandettini PA, Porro CA (2007): Functional responses in the human spinal cord during willed motor actions: Evidence for side- and rate-dependent activity. J Neurosci 27:4182–4190.

Montalban X, Sastre-Garriga J, Filippi M, Khaleeli Z, Tellez N, Vellinga MM, Tur C, Brochet B, Barkhof F, Rovaris M, Miller DH, Polman CH, Rovira A, Thompson AJ. (2009): Primary progressive multiple sclerosis diagnostic criteria: A reappraisal. Mult Scler 15:1459–1465.

Nijeholt GJ, van Walderveen MA, Castelijns JA, van Waesberghe JH, Polman C, Scheltens P, Rosier PF, Jongen PJ, Barkhof F (1998): Brain and spinal cord abnormalities in multiple sclerosis. Correlation between MRI parameters, clinical subtypes and symptoms. Brain 121 (Part 4):687–697.

Oldfield RC (1971): The assessment and analysis of handedness: The Edinburgh inventory. Neuropsychologia 9:97–113.

Pierpaoli C, Jezzard P, Basser PJ, Barnett A, Di Chiro G (1996): 1iffusion tensor MR imaging of the human brain. Radiology 201:637–648.

Riccitelli G, Rocca MA, Pagani E, Rodegher ME, Rossi P, Falini A, Comi G, Filippi M (2011): Cognitive impairment in multiple sclerosis is associated to different patterns of gray matter atrophy according to clinical phenotype. Hum Brain Mapp. Epub ahead of print 2010 Aug 25; doi: 10.1002/hbm.21125.

Rocca MA, Gavazzi C, Mezzapesa DM, Falini A, Colombo B, Mascalchi M, Scotti G, Comi G, Filippi M (2003): A functional magnetic resonance imaging study of patients with secondary progressive multiple sclerosis. Neuroimage 19:1770–1777.

Rocca MA, Colombo B, Falini A, Ghezzi A, Martinelli V, Scotti G, Comi G, Filippi M (2005): Cortical adaptation in patients with MS: A cross-sectional functional MRI study of disease phenotypes. Lancet Neurol 4:618–626.

Rocca MA, Valsasina P, Absinta M, Riccitelli G, Rodegher ME, Misci P, Rossi P, Falini A, Comi G, Filippi M (2010): Default-mode network dysfunction and cognitive impairment in progressive MS. Neurology 74:1252–1259.

Rovaris M, Bozzali M, Santuccio G, Ghezzi A, Caputo D, Montanari E, Bertolotto A, Bergamaschi R, Capra R, Mancardi G, et al. (2001): In vivo assessment of the brain and cervical cord pathology of patients with primary progressive multiple sclerosis. Brain 124 (Part 12):2540–2549.

Rovaris M, Bozzali M, Iannucci G, Ghezzi A, Caputo D, Montanari E, Bertolotto A, Bergamaschi R, Capra R, Mancardi GL, et al (2002): Assessment of normal-appearing white and gray matter in patients with primary progressive multiple sclerosis: A diffusion-tensor magnetic resonance imaging study. Arch Neurol 59:1406–1412.

Smith SM, Zhang Y, Jenkinson M, Chen J, Matthews PM, Federico A, De Stefano N (2002): Accurate, robust, and automated longitudinal and cross-sectional brain change analysis. Neuroimage 17:479–489.

Stroman PW, Krause V, Malisza KL, Frankenstein UN, Tomanek B (2001): Characterization of contrast changes in functional MRI of the human spinal cord at 1.5 T. Magn Reson Imaging 19:833–838.

Stroman PW, Filippi M (2008): Functional MRI of the Spinal Cord, FMRI Techniques, and Protocols. Totowa, NJ: Humana Press.

Thompson AJ, Kermode AG, Wicks D, MacManus DG, Kendall BE, Kingsley DP, McDonald WI (1991): Major differences in the dynamics of primary and secondary progressive multiple sclerosis. Ann Neurol 29:53–62.

Valsasina P, Agosta F, Absinta M, Sala S, Caputo D, Filippi M (2010): Cervical cord functional MRI changes in relapse-onset MS patients. J Neurol Neurosurg Psychiatry 81:405–408.

Vrenken H, Seewann A, Knol DL, Polman CH, Barkhof F, Geurts JJ (2010): Diffusely abnormal white matter in progressive multiple sclerosis: in vivo quantitative MR imaging characterization and comparison between disease types. AJNR Am J Neuroradiol 31:541–548.

Zackowski KM, Smith SA, Reich DS, Gordon-Lipkin E, Chodkowski BA, Sambandan DR, Shteyman M, Bastian AJ, van Zijl PC, Calabresi PA (2009): Sensorimotor dysfunction in multiple sclerosis and column-specific magnetization transfer-imaging abnormalities in the spinal cord. Brain 132 (Part 5):1200–1209.